Neuron, Vol. 12, 571-582, March, 1994, Copyright © 1994 by Cell Press

Association of Poly(A) mRNA with Microtubules in Cultured Neurons

Gary J. Bassell,* Robert H. Singer,† and Kenneth S. Kosik*
*Center for Neurologic Disease
Brigham and Women's Hospital and
Harvard Medical School
Boston, Massachusetts 02115
†Department of Cell Biology
University of Massachusetts Medical Center
Worcester, Massachusetts 01655

Summary

The structural basis for the synthesis of specific proteins within distinct intraneuronal compartments is unknown. We studied the distribution of poly(A) mRNA within cultured cerebrocortical neurons using high resolution in situ hybridization to identify cytoskeletal components that may anchor mRNA. After 1 day in culture, poly(A) mRNA was distributed throughout all of the initial neurites, including the axon-like process. At 4 days in culture, poly(A) mRNA was distributed throughout the cell body and dendritic processes, but confined to the proximal segment of the axon. Poly(A) mRNA was bound to the cytoskeleton as demonstrated by resistance to detergent extraction. Perturbation of microtubules with colchicine resulted in a major reduction of dendritic poly(A) mRNA; however, this distribution was unaffected by cytochalasin. Ultrastructural in situ hybridization revealed that poly(A) mRNA and associated ribosomes were excluded from tightly bundled microtubules.

Introduction

Neurons are highly polarized cells with two morphologically and functionally distinct types of processes: axons and dendrites. Protein synthesis is restricted to the somatodendritic compartment in most neurons; in contrast, most axons are devoid of polysomes (for review see Steward and Banker, 1992). Therefore, axons rely upon the transport of newly synthesized proteins over considerable distances to reach their correct cytological destinations. Dendrites can synthesize proteins where they are required by positioning specific mRNAs at proximal sites. The localization of microtubule-associated protein 2 (MAP2) mRNA in situ and in culture provides one such example (Garner et al., 1988; Bruckenstein et al., 1990; Kleiman et al., 1990). Transport of RNA into dendrites of hippocampal neurons in culture has been demonstrated using ^{3}H[uridine] labeling (Davis et al., 1987). Ultrastructural studies have identified polysomes associated with internal membranes beneath the postsynaptic membrane of dendritic spines (Steward and Levy, 1982; Steward, 1983). Biochemical analysis of these synaptodendrosome fractions have demonstrated that the proteins synthesized are incorporated into synaptic structures (Rao and Steward, 1991). These data provide evidence for the targeting of dendritic mRNA as a mechanism for positioning proteins to their sites of function.

The majority (>85%) of translatable mRNA is bound to the cytoskeleton, whereas untranslated mRNA and monomeric ribosomes are soluble (for reviews see Hesketh and Pryme, 1991; Singer, 1992). The interaction of mRNAs with specific cytoskeletal filament systems could provide a mechanism to localize mRNAs to distinct intraneuronal compartments. Analysis of mRNA-cytoskeletal interactions in nonneuronal cells has identified a major role for the actin cytoskeleton in fibroblasts (Sundell and Singer, 1991; Taneja et al., 1992), muscle (Horne and Hesketh, 1990), epithelia (Ramaekers et al., 1983), and HeLa cells (Lenk et al., 1977; Ornelles et al., 1986). Our objective was to identify cytoskeletal components in neurons that anchor mRNA. To derive general mechanisms for the cytoskeletal localization of mRNA, we focused on the poly(A) sequence, a marker for the 3' end of most mRNAs (Sheiness and Darnell, 1973). Using fluorescence in situ hybridization, the effects of cytoskeletal perturbation on the localization of poly(A) mRNA were evaluated. To visualize directly the attachment of mRNA to a cytoskeletal filament, each was detected using double-label immunogold methods and analyzed by electron microscopy.

Results

Compartmentalization of Poly(A) mRNA in Developing Processes

The use of primary neuronal cultures to study mRNA localization offers distinct advantages to tissue sections, as they permit direct visualization of individual cells and their complete sets of processes. Comparable with the staging of cultured hippocampal neurons (Dotti et al., 1988), most cortical neurons undergo the following developmental sequence: shortly after the neurons have attached to the substrate, they extend actin-rich lamellae (stage 1). These lamellipodia consolidate to form a relatively symmetric array of minor neurites (stage 2). Within the first 24 hr, one of the minor neurites becomes significantly longer than the others and begins to assume the morphology of an axon (stage 3). Within the next few days, the other neurites develop the tapering and branching characteristics of dendrites (stage 4). The compartmentalization of MAP2, which has been well documented in situ and in culture (Matus et al., 1981, 1986; Caceres et al., 1984; Kosik and Finch, 1987), is shown in Figures 1A, 1C, and 1E. At 1 day in culture, MAP2 was distributed throughout the cell body and all of the neurites (Figure 1A). In cortical neurons cultured for 4 days,

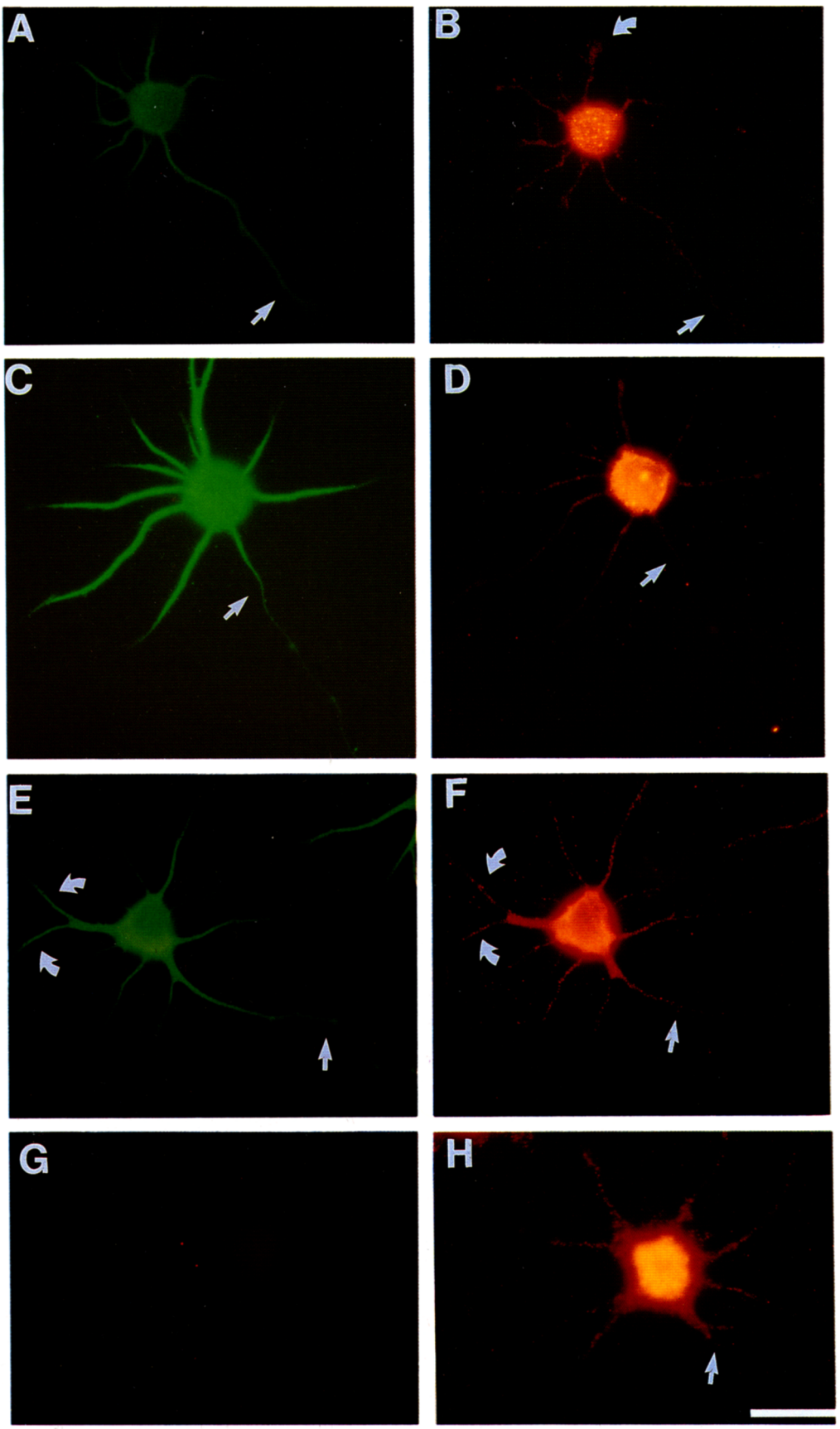
A
B
C
D
E
F
G
H

Table 1. Dendritic Hybridization Signal: Effects of Cytoskeletal Perturbation

	Extent of Hybridization Signal within Individual Dendrites			
			Hybridization Signal	
	Dendrite Length (μm)	Oligo(dT) Signal (μm)	>70% of Process	<30% of Process
No drug	40 ± 3.5	35 ± 3.9	93	0
Cytochalasin	38 ± 2.5	28 ± 1.5	81	0
Colchicine	38 ± 2.1	8 ± 1.2	27	62

Cerebrocortical neurons (4 days after plating) were treated with cytochalasin D or colchicine before fixation. Oligo(dT) hybridization was detected using Cy3-labeled antibody (rhodamine), and MAP2 protein was detected by immunocytochemistry using FITC-labeled antibody. Dendritic lengths were estimated from 100 micrographs by measuring the distance of MAP2 labeling from the origin through dendritic branches. At each branch point, measurement continued along one of the branches. Hybridization was not distributed uniformly throughout the process, unlike MAP2, but present in a speckled fluorescent pattern. This permitted quantitation of the extent to which hybridization was detected throughout the length of the process. Dendritic segments without detectable signal were subtracted from the dendritic length (MAP2 signal). Signal was frequently not detectable within terminal dendrites, and the absence of hybridization signal in these segments was similarly subtracted. The mean dendritic lengths and extent of hybridization signal are indicated below with SEMs. Dendritic hybridization was scored into two categories: hybridization signal observed in >70% of the dendritic length and hybridization signal observed in <30% of total dendritic length. Values shown in both categories are the percentage of neurons examined showing indicated dendritic hybridization signal (mean for three hybridizations).

many neurites exhibited a tapered and branched appearance; a single axon-like process, considerably longer than the others, was nontapering and of finer caliber. MAP2 was enriched in the somatodendritic compartment of these neurons (Figures 1C and 1E).

The distribution of poly(A) mRNA was studied using high resolution fluorescence in situ hybridization. In all neurons, hybridization was greatest in the cell body (Figure 1). Intranuclear hybridization was also occasionally observed in large foci, consistent with previous analysis (Carter et al., 1991). Poly(A) mRNA was detected in a punctate pattern in neuronal processes, and the hybridization pattern suggested a clustered distribution of mRNA (Figure 1). At 1 day in culture, poly(A) mRNA was distributed throughout all of the processes, both in the incipient axon and in the remaining minor neurites (Figure 1B). An analysis of 30 cells revealed 28 with hybridization in every neurite. In the axon-like neurite, hybridization frequently extended throughout the majority of the process (approximately 65 μm) (Figure 1B). However, after 4 days in culture, poly(A) mRNA was concentrated in the somatodendritic compartment (Figures 1D and 1F). From analysis of over 100 cells, greater than 90% exhibited somatodendritic compartmentalization at 4 days in culture. These data suggest that, during development, the density of axonal poly(A) mRNA is not maintained throughout the length of the process, but do not rule out the possibility that lower levels of undetected mRNAs exist in distal axonal segments. Within dendritic processes, strong hybridization to poly(A) mRNA was observed throughout the proximal dendrites, and the fluorescence intensity decreased in a proximodistal gradient (Figures 1D and 1F). Poly(A) mRNA was less abundant after the first dendritic branch point, but clusters of hybridization signal were observed in distal segments (Figure 1F). Quantitation of the distance which hybridization signal extended into dendrites suggests that, in the majority of neurons, poly(A) mRNA is detectable in >70% of the process length (Table 1). The concentration of hybridization intensity within proximal dendrites could be explained by the tapering of the process. Electron microscopic data obtained by reconstruction of serial sections of pyramidal dendrites have shown that the dendritic diameter of preterminal segments was up to 8 times larger than that of terminal segments (Hillman, 1988). In cultured hippocampal neurons, dendritic diameters have been estimated from electron micrographs to taper approximately 5-fold (Bartlett and

Figure 1. Intraneuronal Distribution of MAP2 and Poly(A) mRNA

Double-label detection of poly(A) mRNA and MAP2 by in situ hybridization and immunofluorescence.

(A and B) One day cortical neuron. (A) MAP2 distribution. (B) Detection of poly(A) mRNA at termini of dendritic processes (curved arrow). Detection of poly(A) mRNA in the axon-like process (arrow).

(C and D) Cortical neuron cultured for 4 days. (C) MAP2 distribution; note the decrease in immunoreactivity observed along the axonal process (arrow). (D) Poly(A) mRNA is concentrated to the somatodendritic compartment. Hybridization is detected in the proximal segment of the axonal process (arrow).

(E and F) Cortical neuron cultured for 4 days. (E) MAP2 localization in dendritic branches (curved arrows). Decrease in MAP2 immunoreactivity detected in distal axonal segments (arrow). (F) Poly(A) mRNA detection after a dendritic branch point (curved arrows) and in the proximal segment of the axon (arrow).

(G) Background hybridization to a cortical neuron cultured for 4 days using a control oligo(dA) (digoxigenin) probe detected using Cy3-labeled antibody.

(H) Detection of poly(A) mRNA in cortical neurons extracted for 1 min with 0.2% Triton X-100 in cytoskeletal buffer prior to fixation. Poly(A) mRNA is retained in the cell body and proximal dendrites. Arrow, axonal process.

Bar, 25 μm.

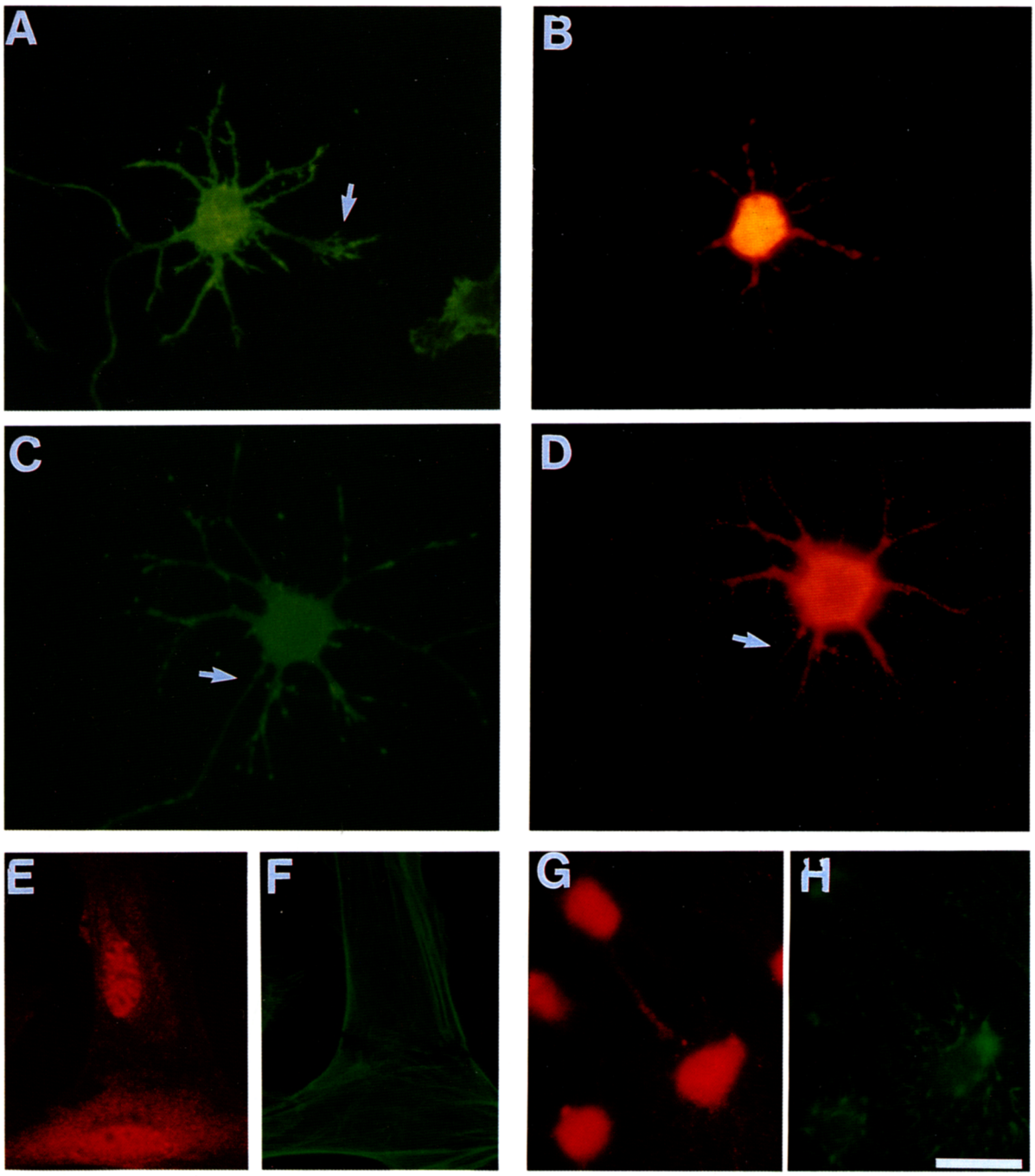

Figure 2. Distribution of Actin and Poly(A) mRNA following Treatment with Cytochalasin D

Cerebrocortical cultures (4 days after plating) were treated with cytochalasin D (5 μg/ml) in N2 media for 1 hr prior to fixation.
(A and B) Untreated cortical neuron double labeled for actin (green) and poly(A) mRNA (red). Actin labeling using FITC-labeled phalloidin (Molecular Probes) showed a filamentous distribution within growth cones (arrow) and the presence of microspikes. Oligo(dT) hybridization is concentrated in the cell body and dendritic processes.
(C and D) Cytochalasin D–treated neuron showing a diffuse distribution of actin (green) with occasional bright spots of fluorescence in processes. Note the loss of filamentous morphology from dendritic terminus. Poly(A) mRNA (red) is distributed throughout the cell body and dendritic processes. Arrows, axonal process.
(E) Oligo(dT) hybridization in Triton-extracted nonneuronal cells detected poly(A) mRNA within nuclei and cytoplasm.
(F) Same cell as in (E), showing labeling of actin stress fibers.
(G) Oligo(dT) hybridization in cytochalasin D–treated nonneuronal cells exhibited a marked loss of poly(A) from the cytoplasm.
(H) Same field as in (G), showing labeling of disrupted actin filaments.
Bar, 20 μm.

Banker, 1984). Therefore, the hybridization signal along the z-axis (perpendicular to the process) would be expected to decrease in a proximodistal gradient.

Although poly(A) mRNA was not detectable in the majority of the axon after 4 days in culture, most neurons contained poly(A) within the proximal segment of the axon (Figures 1D and 1F, arrows). The length of the proximal segment that contained poly(A) mRNA ranged from 2 to 10 μm, whereas the entire axonal process was over 150 μm. Hybridization with control oligo(dA) probes (digoxigenin labeled) showed low background throughout the cell and did not reveal fluorescent signal in dendritic processes (Figure 1G). Neuronal cultures extracted with 0.2% Triton X-100 in hypertonic buffer exhibited strong hybridization (Figure 1H), demonstrating that poly(A) mRNA within the cell body and proximal dendrites was bound to the cytoskeleton.

Effects of Microfilament Perturbation on the Distribution of Poly(A) mRNA

Cytochalasins have been previously used to disrupt microfilaments in neurons (Letourneau et al., 1987; Forscher and Smith, 1988) and to release mRNA from the actin cytoskeleton (Ornelles et al., 1986; Sundell and Singer, 1991; Taneja et al., 1992). Cortical neurons (4 days in culture) were treated with 5 μg/ml cytochalasin D for 1 hr prior to fixation and hybridization. The cytochalasin dose used here was 10-fold above that used to disrupt mRNA localization in nonneuronal cells (Sundell and Singer, 1991; Taneja et al., 1992). Fluorescein isothiocyanate (FITC)–phalloidin labeling revealed the presence of actin throughout the cell body and processes. Filamentous actin was most evident within flattened growth cones (Figure 2A, arrow). Following cytochalasin treatment, there was a perturbation in the distribution of neuronal actin, most evident as a loss of filamentous actin bundles from dendritic growth cones (Figure 2C). The distribution of actin following cytochalasin treatment was diffuse, although some bright fluorescent spots were observed within processes (possible aggregates of actin) (Figure 2C). The polar morphology of the neuron remained intact, and poly(A) mRNA remained in dendritic processes, in a proximodistal gradient of decreasing signal intensity, and remained confined to the proximal segment of the axon (Figure 2D; Table 1). Poly(A) mRNA was also retained in neurites after 1 day in culture following cytochalasin D treatment (data not shown). Therefore, the localization of the majority of poly(A) mRNA within neuronal processes was not dependent on the integrity of microfilaments. There was no evidence of an alteration in the distribution of poly(A) mRNA within the cell body; however, it may be necessary to Triton extract neurons following cytochalasin D treatment to eliminate hybridization to soluble mRNA, which was released from microfilaments but still present in the cell body (region of greatest volume). However, because of the fragility of neuronal cytoskeletons, only the healthiest cultures will resist the Triton extraction. Prior treatment with cytoskeletal perturbing drugs adds further complications to this procedure, and it cannot be determined as yet whether poly(A) mRNA within the neuronal cell body is bound to actin, as has been reported for other non-process-bearing cells. However, non-process-bearing cells present in the neuronal cultures were found to have actin-associated poly(A) mRNA by comparison of hybridization in untreated and cytochalasin D-treated cells which were Triton extracted (Figures 2E and 2G). In these cells, cytochalasin D treatment resulted in a dramatic perturbation of actin stress fibers (Figures 1F and 1H). The sensitivity of nonneuronal mRNA to cytochalasin D was comparable with that observed previously in fibroblasts (Taneja et al., 1992).

Effects of Microtubule Perturbation on the Distribution of Poly(A) mRNA

Since poly(A) mRNA was unaffected by perturbation of microfilaments, we then investigated microtubules for their role in mRNA anchoring. Cortical neurons (4 days in culture) were treated with 10 μg/ml colchicine for 1 hr prior to fixation and hybridization. The distribution of tubulin in the cell body of colchicine-treated neurons was less fibrillar, and the caliber of the processes was significantly reduced (Figure 3A). Important to the preservation of neuronal morphology was the brief time of drug exposure (1 hr), thereby minimizing perturbation to other cytoskeletal components. For example, the distribution of actin following colchicine treatment was similar to that observed previously without exposure to drug (Figure 3B). However, 62% of the neurons showed a major loss of poly(A) mRNA in their dendrites (Table 1); most dendritic processes had no detectable hybridization (Figures 3A and 3B, inset). In the majority of neurons, poly(A) mRNA was also lost from the proximal segment of the axon. In cultures treated with colchicine 1 day after plating, hybridization was significantly reduced in all minor neurites (data not shown). The depolymerization of colchicine labile microtubules was likely to account for the reduction in hybridization intensity within neuronal processes, suggesting a microtubule dependency in the anchoring of poly(A) mRNA. The depolymerization of microtubules may permit poly(A) mRNA to diffuse into the cell body (region of greatest volume). Alternatively, poly(A) mRNA, which was originally associated with dendritic microtubules, may be degraded. A subset of cortical neurons (27%) (Table 1) did not exhibit colchicine-induced alterations in process morphology or dendritic mRNA distribution, suggesting drug-stable populations (Goldschmidt and Steward, 1982). The inability to release dendritic poly(A) mRNA from these neurons (Table 1) might be explained by a population of colchicine-resistant microtubules (Ferreira et al., 1989).

Owing to the known interactions between microtu-

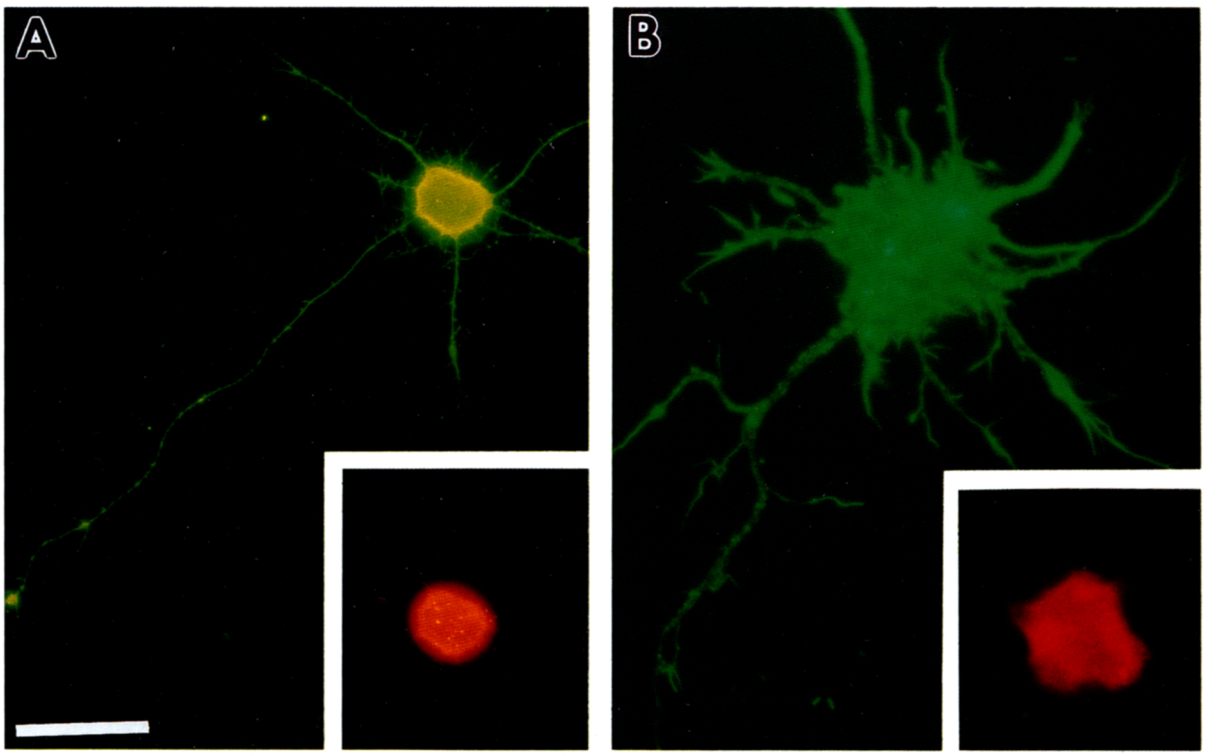

Figure 3. Reduction in Dendritic Poly(A) mRNA following Colchicine Treatment

Cerebrocortical cultures were treated with colchicine (20 μg/ml) in N2 media for 1 hr before fixation. Detection of digoxigenin-labeled oligo(dT) probe with Cy3 (red) and cytoskeletal proteins with FITC (green).

(A) Four day cortical neuron. Labeling with monoclonal antibody to tubulin (Amersham). Poly(A) mRNA (inset) is confined to the cell body, and a marked loss of dendritic hybridization was observed.

(B) Five day cortical neuron. Labeling for actin using phalloidin. The majority of dendritic processes exhibited reduced hybridization with the oligo(dT) probe (inset).

Bar, 25 μm.

bules and intermediate filaments, it was possible that the localization of poly(A) mRNA within dendrites depended upon the integrity of intermediate filaments. The effects of colchicine on intermediate filaments have been demonstrated in nonneuronal cells, where vimentin filaments collapse around the nucleus into tight perinuclear coils (Goldman, 1971). Cortical neurons cultured for 4 days demonstrated weak immunofluorescence with antibodies to vimentin or neurofilament proteins, suggestive of a paucity of intermediate filaments (data not shown). These results are consistent with previous immunofluorescence observations that vimentin is expressed only early in culture, followed by the appearance of neurofilament proteins NF-M and NF-L at 4 days and NF-H at 2 weeks (Shaw et al., 1985). At the ultrastructural level, intermediate filaments were infrequent after 2 weeks in culture (Bartlett and Banker, 1984). The distribution of intermediate filaments in cortical neurons was not observed to collapse over the nucleus following colchicine treatment (data not shown). These data suggest that intermediate filaments in these developing cortical neurons are unlikely to be responsible for the observed reduction in dendritic poly(A) mRNA following colchicine treatment. Further work is needed to determine whether intermediate filaments are involved in mRNA localization at later stages.

Ultrastructural Visualization of Poly(A) mRNA Association with Microtubules

To visualize the poly(A) mRNA–cytoskeletal association directly, we utilized ultrastructural in situ hybridization methods combined with immunogold labeling (for review see Bassell, 1993). Detection of poly(A) mRNA and the neural-specific isotype of β-tubulin (class III) (Burgoyne et al., 1988) in Triton-extracted cultures demonstrated that the majority of hybridization in each cell was associated with microtubules. This conclusion was based on the following observations; the majority (55%) of the poly(A) mRNA signal within neuronal processes was less than 50 nm from anti-tubulin binding (Table 2; Figure 4). Less than 5% of the poly(A) mRNA signal was at distances greater than 100 nm. Within the cell body, 45% of the hybridization signal was within 50 nm of tubulin; however, some signal was also observed at distances over 100 nm (Table 2). The proximity between the different sized gold particles in thin sections (50 nm thickness)

Table 2. Ultrastructural Colocalization with Microtubules

	Distance between Oligo(dT) (12 nm Particles) and Microtubules (6 nm Particles)		
	<50 nm	50–100 nm	>100 nm
Neuronal process	55	42	3
Cell body	45	37	18
Nonneuronal	13	20	67

Cortical neurons (4 days in culture) were Triton extracted in cytoskeletal buffer and fixed as described in the Experimental Procedures. Oligo(dT) (digoxigenin) probes were detected using 12 nm gold-conjugated antibodies, and class III tubulin was detected using a monoclonal antibody and a 6 nm gold-labeled secondary antibody. The hybridization signal was evident as clusters of 12 nm particles, i.e., 3 particles per cluster (see Figure 4). Clusters of 12 nm gold were considered as individual hybridization signals to avoid the possibility of scoring a single mRNA molecule more than once. One hundred signals (from 6 cells) were photographed at 50,000× using a JEOL 1200EX transmission electron microscope. The distance between oligo(dT) hybridization signals (12 nm particle) and the nearest 6 nm particle (tubulin) was measured in neuronal processes and cell bodies. Similar analysis was performed on non-neuronal cells that did not have processes. These nonneuronal cells were obtained by trypsinization of cortical cells and plating on uncoated coverslips; under these conditions, neurons do not attach. Nonneuronal tubulin was detected using a monoclonal antibody to α-tubulin, which was not cell-type specific.

of Triton-extracted cells strongly suggests a nonrandom coincidence between poly(A) mRNA and microtubules.

Poly(A) mRNA was not observed to be associated with tightly bundled microtubules, with intermicrotubular distances less than 50 nm (Figures 4C–4E). This was not attributed to a paucity of tightly bundled microtubules, as bundles were frequently observed (Figures 4C–4E). It was frequently possible to measure intermicrotubule distances at sites of hybridization if the filaments were positioned within the plane of sectioning and optimally stained with heavy metals. Only 10% of these poly(A) mRNA signals (cluster of 12 nm gold particles) localized to microtubules spaced apart by <50 nm. The majority of poly(A) was associated with the following types of microtubules: parallel microtubules (average intermicrotubule distance of 80 nm; n = 25 hybridization signals), microtubules intersecting at branched angles (nonparallel), and individual microtubules (this association may be attributed to thin sectioning). In dendritic regions that contained both tightly bundled and loosely spaced microtubules, poly(A) mRNA was preferentially localized to the looser arrangements (Figures 4C–4E). Poly(A) mRNA was also excluded from those microtubules that were tightly bundled in the proximal segment of the axon (data not shown).

The hybridization signal (12 nm gold particles) near microtubules was in the form of clusters of gold particles (2–6 particles per cluster), and multiple clusters were observed in proximity (Figures 4A–4E). These data suggest that multiple poly(A) mRNA molecules may be aggregated at cytoskeletal attachment sites between microtubules. The ultrastructural approach permitted the morphologic identification of polysomes, present as electron dense clusters of circular particles (Figure 4A). This identification was confirmed by the disappearance of these clusters (polysomes) when cells were treated with puromycin, which inhibits ribosome initiation and disengages ribosomes from mRNA (data not shown). Poly(A) mRNA molecules were frequently observed in clusters colocalized with polysomes (Figure 4A), suggesting that the detected mRNAs were being translated.

To support the above observations, two controls were performed. Nonspecific binding of digoxigenin-labeled oligo(dA) probes showed very low background levels of gold particles and did not colocalize with microtubules (electron microscopy data not shown). Oligo(dT) (digoxigenin) probes hybridized to nonneuronal cells (without processes) did not exhibit frequent interactions with microtubules labeled with antibody to all β-tubulin isotypes (Figure 4F; Table 2), and mRNA was not released from the cytoskeleton following colchicine treatment and Triton extraction (data not shown). These data are consistent with previous reports in fibroblasts, where interactions of mRNA with microtubules were not observed (Singer et al., 1989; Sundell and Singer, 1991; Taneja et al., 1992).

Discussion

In neurons, the mRNA population has not previously been visualized with high resolution, nor have specific cytoskeletal elements that could account for mRNA compartmentalization been identified. Here, we have shown that dendritic localization of poly(A) mRNA requires microtubules. It has been proposed that mRNA localization involves a two-step process (Yisraeli et al., 1990): the transport of newly synthesized mRNA from its entrance into the cytoplasm to its region of localization and the subsequent anchoring of that mRNA to prevent its diffusion. An alternative hypothesis is that mRNAs diffuse into dendrites and are then anchored to specific dendritic cytoskeletal components. Recent microinjection experiments of fluorescently labeled myelin basic protein mRNA have permitted kinetic analysis of mRNA localization in oligodendrocytes, which occurs at rates comparable with fast transport (Ainger et al., 1993). These data provide evidence that support an active role of the cytoskeleton in both transport and anchoring. The microscopic data obtained here provide information on the steady-state distribution of mRNA and permit visualization of total cytoskeleton-associated mRNA. This study provides the first evidence for an involvement of microtubules in the localization of endogenous mRNA in a somatic cell. Microtubules have been previously shown to be involved in the localization of untranslated maternal mRNA in oocytes. In Xenopus

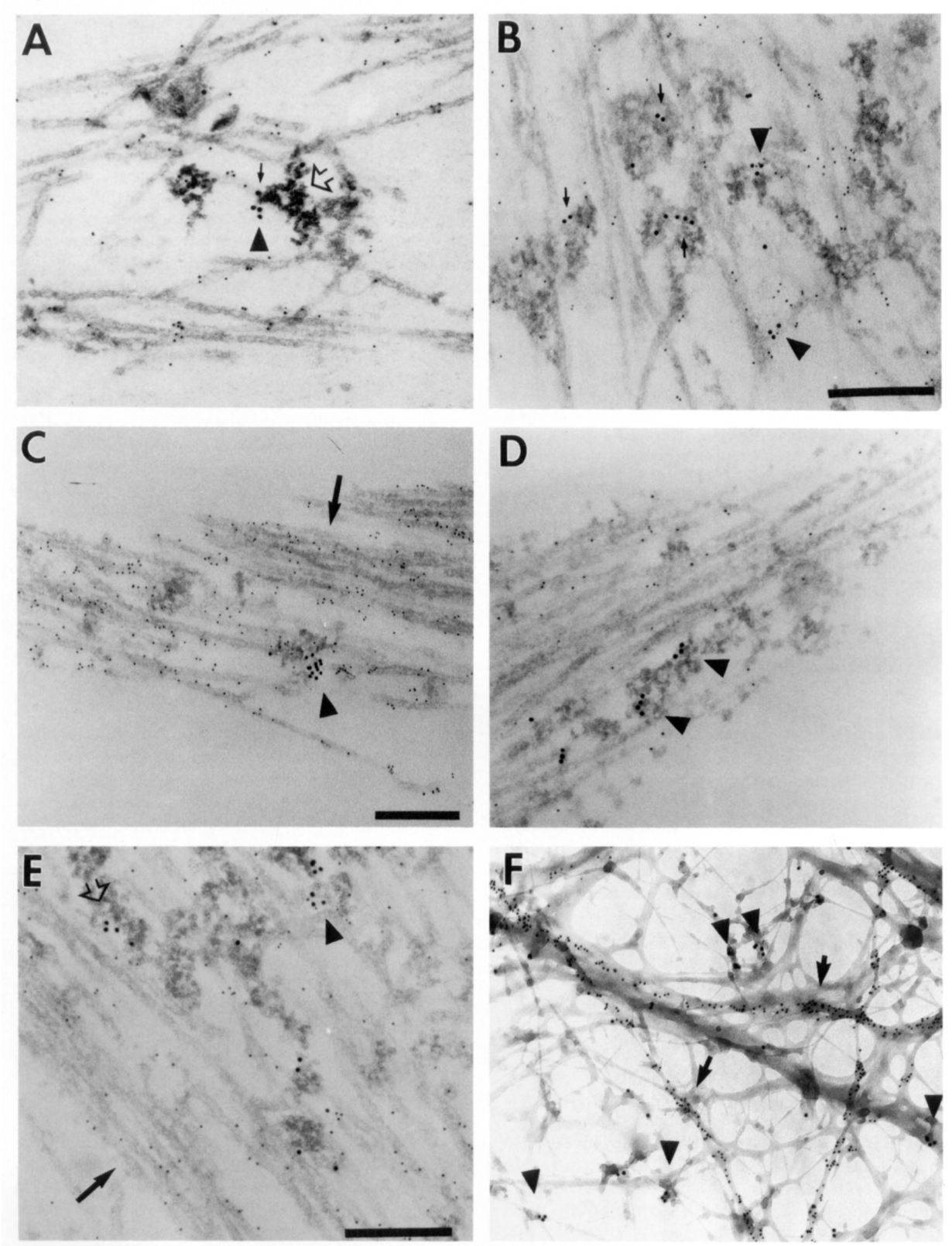

Figure 4. Ultrastructural Localization of Poly(A) mRNA

Double-label detection of poly(A) mRNA (12 nm gold particles) and class III tubulin (6 nm gold) in thin sections of Triton-extracted cerebrocortical neurons from 4-day-old cultures.

(A) Poly(A) mRNA (arrowhead) at the junction between the cell body and a dendritic process was associated with a labeled microtubule (arrow). Morphologically preserved polysomes are present at sites of hybridization (open arrow).

oocytes, the translocation of *veg-1* RNA to the vegetal pole required intact microtubules, whereas the anchoring of *veg-1* RNA within the vegetal pole could be perturbed by microfilament depolymerization (Yisraeli et al., 1990). In Drosophila nurse cells and oocytes, bicoid mRNA transport and anchoring were dependent on microtubules (Pokrywka and Stephenson, 1991). Digital imaging analysis has suggested that microinjected MBP mRNA in oligodendrocytes formed granules which were near microtubules (Ainger et al., 1993). The peripheral localization of β-actin mRNA in fibroblasts was observed to be solely dependent on microfilaments (Sundell and Singer, 1991).

The mechanism of dendritic mRNA transport could involve localization of mRNA on microtubules. Axonal microtubules are of uniform polarity with their plus ends oriented distally (Burton and Paige, 1981; Heidemann et al., 1981), whereas dendrites have a mixed microtubule orientation (Baas et al., 1988). Therefore, the translocation of mRNA along microtubules with minus end distal polarity could explain the concentration of mRNA within dendrites and not axons (Black and Baas, 1989). However, the presence of poly(A) mRNA in minor neurites (Figure 1B) and the proximal segment of axonal processes (Figures 1D and 1F), which have microtubules with plus ends distal to the cell body (Baas et al., 1989), suggest that attachment of mRNA only to microtubules with distal minus ends may not be the only mode of attachment. If microtubule polarity is involved in mRNA localization within neuronal processes, it may be that both types of microtubule orientation are utilized to permit localization of specific dendrite- and axon-directed populations. Although most mRNAs are not detected in mature axons, in situ hybridization analyses have detected the presence of tau mRNA in proximal segments (Litman et al., 1993) and vasopressin and oxytocin mRNAs in axons of the hypothalamo–neurohypophysial tract (Jirikowski et al., 1990; Mohr et al., 1991). In this study, poly(A) mRNA was detected in axons, although concentrated in proximal segments during development (Figure 1). The active transport of mRNAs into dendrites and/or axons could involve microtubule-associated motor proteins that move specifically toward plus or minus ends of microtubules. Several proteins belonging to either kinesin or dynein families which produce force in preferred directions along microtubules have been identified (Vale, 1992), but none have yet been implicated in mRNA movement.

Anchoring to microtubules may involve the direct binding of mRNAs to tubulin; however, this mechanism would have limited capacity to specify localization to multiple neuronal domains, since tubulin is distributed throughout the neuron. A more plausible mode of attachment might involve binding to microtubule-associated proteins (MAPs), which have been shown to exhibit regional localization within the neuron. The ultrastructural distribution of poly(A) mRNA on microtubules was suggestive that mRNA may not be directly bound to the microtubule, but instead bound to associated proteins between adjacent microtubules. Support for this observation is that hybridization was not uniformly distributed or directly localized on the surface of microtubules, as was observed with an antibody to tubulin. This pattern is similar to previous ultrastructural studies, which have shown that immunogold labeling of MAP2 and MAP1B was distributed between microtubules in clustered arrangements and not distributed linearly along microtubules (Hirokawa et al., 1988; Sato-Yoshitake et al., 1989). Poly(A) mRNA was frequently present between loosely spaced microtubules and did not make physical contact with the tubule. Supportive of the above hypothesis, in vitro data have shown that isolated preparations of MAPs, but not tubulin by itself, bind poly(A) mRNA (Schroder et al., 1982, 1984). It would be worthwhile to develop further in situ hybridization methodology that permits visualization of additional cellular structures involved in mRNA localization. For example, quick-freezing approaches have identified that immunogold labeling of MAPs is observed at cross bridges between microtubules, whereas thin section analysis of Triton-extracted and resin-embedded neurons has only revealed the presence of "fuzzy" structures which colocalize with MAPs (Sato-Yoshitake et al., 1989).

Previous studies have concluded that the majority of mRNAs are not detected in axons, and it is generally believed that most proteins are not synthesized in axons (Steward and Banker, 1992). However, the possibility always existed that the detection methods used lacked the sensitivity to detect low levels of mRNA. In 1 day cortical cultures, poly(A) mRNA was detected throughout the majority (>80%) of the axon-like process; therefore, the in situ hybridization method used was sensitive enough to detect axonal poly(A) mRNA. In contrast, after 4 days in culture, poly(A) mRNA was not detected in the majority (>90%) of the axonal process and confined to the proximal segment. One explanation for the progressive loss of axonal hybridization is that the majority of newly synthesized poly(A) mRNA is excluded from entering the axon at some point in development. Alternatively, poly(A) mRNA

(B) Dendritic poly(A) mRNA molecules (arrows) observed between parallel series of microtubules. Clusters of poly(A) mRNA (arrowheads) juxtaposed to sites of anti-tubulin binding.
(C–D) Dendritic poly(A) mRNA (arrowheads) was not associated with tightly bundled microtubules (arrows).
(E) Poly(A) (open arrow) at the edge of bundled microtubules (arrow). Poly(A) and tubulin (arrowhead).
(F) Labeling of nonneuronal tubulin (arrows) in a whole-mount preparation. Poly(A) mRNA (arrowheads) was associated with filaments that were unlabeled by anti-tubulin. Bar, 200 nm.

may enter the axon but get rapidly degraded. In favor of the exclusion hypothesis, poly(A) mRNA within the proximal segment of the axon was associated with microtubules, yet excluded from tightly packed microtubule bundles in neurons cultured for 4 days (data not shown). As a function of distance from the cell body, poly(A) mRNA declines distally along the axonal process, concommitant with an increase in the density of tightly bundled microtubules. If poly(A) mRNA is bound to certain MAPs, and not to tubulin directly, then the exclusion of most poly(A) mRNA from axons may occur by the absence of those MAPs from tightly bundled axonal microtubules. Alternatively, the bundling of microtubules may sterically prevent or limit the ability of large mRNP complexes from entering certain compartments by preventing access to the microtubule except along the edge of the bundle. It would be interesting to know whether the microtubules in the incipient axon of neurons cultured for 1 day contain loosely spaced microtubules, but it is difficult to distinguish axonal from dendritic processes in thin sections at this early stage in culture. Supportive of this hypothesis, an ultrastructural study on ribosomal distribution in unextracted neurons suggested that bundling of microtubules in the axon may be involved in the confinement of ribosomes within the perikarya (Baas et al., 1987).

Our results demonstrate a major interaction between poly(A) mRNA and the microtubular cytoskeleton in neurons. Further work is needed to identify whether other filament systems also participate in neuronal mRNA localization. For example, it is possible that mRNAs which are anchored within the cell body are not bound to microtubules. In this model, microtubules within the cell body would serve as tracks for only those mRNAs destined for the processes. Alternatively, microtubules could be the only filament system involved in mRNA localization within neurons, and specific interactions with distinct microtubule subpopulations and their associated proteins could provide for sorting to specific regions. Identification of an mRNA–microtubule interaction in neurons should focus further efforts on the mechanisms responsible for the transport and anchoring of distinct species of mRNA to their appropriate domains within the neuron and the mechanism that restricts the majority of mRNA from entering the axon during development.

Experimental Procedures

Cell Culture

The method of neuronal culture has been described in detail by Banker (for review see Goslin and Banker, 1991) and modified for use with cortical neurons in our laboratory (Kosik and Finch, 1987). Cerebral cortex was dissected from embryonic day 18 rats and digested with 0.25% trypsin in Hanks' balanced salt solution. Tissue was washed twice in Hanks' balanced salt solution, placed in modified Eagle's medium with 10% fetal calf serum, and mechanically dissociated by pipetting. Neurons were plated at low density (1000 cells per cm^2) on poly-L-lysine-coated coverslips (1.0 mg/ml; overnight). After neurons had attached to the substrate (2 hr), coverslips were inverted onto a monolayer of astrocytes. The coculture of neurons with glia using this sandwich technique has been previously observed to promote neuronal development. Astrocytes were prepared from postnatal day 1 rat cortex by culturing dissociated cortex in modified Eagle's medium with 10% fetal calf serum on untreated tissue culture plates. Under these conditions, neurons will not attach to the substrate, and the major cell type cultured is the glial fibrillary acidic protein-positive type-1 astrocyte. The coculture was maintained in glutamate-free modified Eagle's medium with N2 supplements, which include transferrin (100 μg/ml), insulin (5 μg/ml), progesterone (20 nM), putrescine (100 μM), and selenium dioxide (30 nM). In addition, extra glucose (600 mg/l), sodium pyruvate (1 mM), and ovalbumin (0.1%) were used.

Drug Treatments/Fixation

To depolymerize microfilaments, cells were treated with 5 μg/ml cytochalasin D (Sigma Chemical Co.) in culture media for 1 hr prior to fixation. To depolymerize microtubules, cells were treated with colchicine (10 μg/ml) (Sigma Chemical Co.) in culture media for 1 hr before fixation. Stock solutions of cytochalasin D and colchicine were made up in dimethyl sulfoxide and ethanol, respectively, and the concentration of these solvents was diluted below 0.1% in the culture media, as not to be toxic to neurons. Neurons attached to coverslips were fixed in paraformaldehyde (4% in phosphate-buffered saline with 5 mM $MgCl_2$) at 1 and 4 days after plating. Some samples (not exposed to drugs) were extracted with 0.2% Triton X-100 in cytoskeletal buffer (0.1 M NaCl, 0.3 M sucrose, 10 mM PIPES, 3 mM $MgCl_2$, 10 μM leupeptin, 2 mM phenylmethylsulfonyl fluoride, 2 mM vanadyl ribonucleoside complex, 2 mM EGTA [pH 6.9]) for 1 min at 4°C and fixed in 4% paraformaldehyde (phosphate-buffered saline) for 15 min. This extraction procedure has been widely used to study the association of mRNA with the cytoskeleton (Taneja et al., 1992). Samples that were processed for electron microscopy were fixed in 2% paraformaldehyde, 0.2% glutaraldehyde (phosphate-buffered saline) following extraction.

Probe Preparation

Synthetic oligo(dT) (55 nucleotides) and oligo(dA) (55 nucleotides) were 3' end labeled with digoxigenin-11-dUTP (Boehringer Mannheim) using terminal transferase (25 pM oligo, 25 mM digoxigenin dUTP, 140 mM potassium cacodylate, 30 mM Tris-HCl [pH 7.6], 1 mM $CoCl_2$, 0.1 mM dithiothreitol, 100 U of terminal transferase) at 37°C for 1 hr. Probes were purified using a 20 ml G-50 column, and the collected fractions were blotted onto nitrocellulose and detected using an anti-digoxigenin–alkaline phosphatase conjugate (Boehringer Mannheim). Positive fractions were lyophilized, resuspended, and combined, and the optical density was measured.

Hybridization

Cells were washed in phosphate-buffered saline (5 mM $MgCl_2$) and then equilibrated in 15% formamide (Sigma Chemical Co.) 2× SSC and 10 mM sodium phosphate (pH 7.0) at room temperature for 10 min. Five nanograms of probe was dried down with Escherichia coli tRNA (10 μg) and sonicated salmon sperm DNA (10 μg) and then suspended in 10 μl of 30% formamide containing 20 mM sodium phosphate (pH 7.0). Probes were mixed with 10 μl of hybridization buffer (20% dextran sulfate, 4× SSC, 0.4% bovine serum albumin, 20 mM sodium phosphate [pH 7.0]). Coverslips were placed cell side down on parafilm containing 20 μl of probe mixture and hybridized for 1.5 hr at 37°C. After hybridization, coverslips were washed for 20 min in 15% formamide 2× SSC at 37°C and three 10 min washes in 1× SSC on a rotary shaker at room temperature.

Immunocytochemistry

Probes were detected using affinity purified sheep antibody to digoxigenin conjugated to horseradish peroxidase (Boehringer Mannheim) and affinity purified goat antibody to horseradish peroxidase conjugated to Cy3 (Jackson Immunoresearch). Cy3, which is brighter than rhodamine, has nearly identical excitation

and emission spectra and was visualized with a rhodamine filter. Owing to higher Cy3 emission at lower wavelengths, background levels of Cy3 fluorescence were occasionally observed using the fluorescein filter. Better fluorochrome separation was achieved using an FITC filter equipped with an emission barrier between 520–560 nm. Immunofluorescence detection of MAP2 was performed simultaneously using monoclonal antibodies to high molecular weight MAP2 (clones AP14-22 obtained from Lester Binder) and affinity purified donkey antibody to mouse IgG conjugated to fluorescein (Jackson Immunoresearch). Microtubules were detected using a monoclonal antibody to tubulin (Amersham) and fluorochrome-conjugated secondary antibody. Actin was detected using FITC-labeled phalloidin (Molecular Probes). FITC fluorescence was not observed using the rhodamine filter (Figure 1). Antibody incubations were for 1 hr at 37°C in Tris-buffered saline with 1% bovine serum albumin and 0.1% Triton X-100 and were followed by several washes in buffer on a rotary shaker. Immunofluorescence was viewed using a Zeis-Axioplan microscope equipped with a 63× Plan-Neofluar objective.

For analysis of dendritic hybridization intensity (Table 1), neurons were randomly selected under the fluorescein filter that displayed immunostaining for MAP2. After each selection, the cartridge was then shifted to the rhodamine filter to visualize poly(A) mRNA. Cells were photographed under both fluorescein and rhodamine filters. Dendritic length was estimated from micrographs by the length of MAP2 labeling (FITC filter). Each process was divided into 2 μm segments, and the presence or absence of poly(A) mRNA signal (rhodamine filter) was indicated. Processes with hybridization signal in >70% of the segments were scored as having a high dendritic hybridization intensity. Absence of signal in >30% of the segments was scored as having low hybridization intensity.

For electron microscopy, oligo(dT) (digoxigenin) probes were detected using the same antibodies to digoxigenin used for light microscopy, but conjugating 12 nm gold to the secondary antibody (Jackson Immunoresearch). To label neuronal microtubules simultaneously, a monoclonal antibody (JuJ1; obtained from Anthony Frankfurter) to the neural-specific isotype of β-tubulin (class III) was detected using 6 nm gold-conjugated secondary antibody.

Controls

For in situ hybridization, control digoxigenin oligo(dA) probes were hybridized in parallel to oligo(dT) in all experiments. Both oligo(dT) and oligo(dA) hybridizations were evaluated by light and electron microscopy and demonstrated low levels of nonspecific hybridization. As an alternative control, hybridization signal could be eliminated when digoxigenin-labeled oligo(dT) probes were hybridized in competition with excess unlabeled oligo(dT) (data not shown).

Electron Microscopy

After rinsing in distilled H_2O, samples were dehydrated to absolute ethanol through a series of graded ethanol. After treatment with propylene oxide poly/bed 812 (1:1) for 30–60 min at room temperature, samples were placed into 100% Epon for 1 hr at room temperature. Beem capsules were filled with fresh 100% poly/bed 812 and quickly inverted onto the surface of the coverslips and polymerized for 48 hr at 60°C. To remove the Beem capsules from the coverslip, samples were immersed in liquid nitrogen for a few seconds and gently tapped to remove the Beem capsule. Thin sections (60–80 nm) were stained with uranyl acetate (1.5% in 50% ethanol) and Reynold's lead citrate for 3 and 5 min, respectively. Samples were thin sectioned parallel to the monolayer, and dendritic and axonal processes were identified at low magnification with a transmission electron microscope (JEOL 1200EX), and various regions were photographed at 50,000×.

Acknowledgments

We would like to thank Adrianna Ferreira for extensive assistance with neuronal cultures and numerous helpful discussions. We thank Lester Binder for antibodies to MAP2 and Anthony Frankfurter for antibody to class III tubulin. We thank Christine Powers and Peter Paskovitch for electron microscopy assistance. This work was supported by a grant from the Alzheimer's Disease and Related Disorders Association to G. J. B. and National Institutes of Health grants AG06601 and NS29031 to K. S. K.

The costs of publication of this article were defrayed in part by the payment of page charges. This article must therefore be hereby marked "*advertisement*" in accordance with 18 USC Section 1734 solely to indicate this fact.

Received August 5, 1993; revised December 10, 1993.

References

Ainger, K., Avossa, D., Morgan, F., Hill, S. J., Barry, C., Barbarese, E., and Carson, J. H. (1993). Transport and localization of exogenous MBP mRNA microinjected into oligodendrocytes. J. Cell Biol. *123*, 431–441.

Baas, P. W., Sinclair, G. I., and Heidemann, S. R. (1987). Role of microtubules in the cytoplasmic compartmentation of neurons. Brain Res. *420*, 73–81.

Baas, P. W., Deitch, J. S., Black, M. M., and Banker, G. A. (1988). Polarity orientation of microtubules in cultured hippocampal neurons: uniformity in the axon and not in the dendrite. Proc. Natl. Acad. Sci. USA *85*, 8335–8338.

Baas, P. W., Black, M. M., and Banker, G. A. (1989). Changes in microtubule polarity orientation during the development of hippocampal neurons in culture. J. Cell Biol. *109*, 3085–3094.

Bartlett, W. P., and Banker, G. A. (1984). An electron microscopic study of the development of axons and dendrites by hippocampal neurons in culture. J. Neurosci. *4*, 1944–1965.

Bassell, G. J. (1993). High resolution distribution of mRNA within the cytoskeleton. J. Cell. Biochem. *52*, 127–133.

Black, M., and Baas, P. W. (1989). The basis of polarity in neurons. Trends Neurosci. *12*, 211–214.

Bruckenstein, D. A., Lein, P. J., Higgins, D., and Fremeau, R. T., Jr. (1990). Distinct spatial localization of specific mRNAs in cultured sympathetic neurons. Neuron *5*, 809–819.

Burgoyne, R. D., Cambray-Deakin, M., Lewis, S., Sarkar, S., and Cowan, N. (1988). Differential distribution of β-tubulin isotypes in cerebellum. EMBO J. *7*, 2311–2319.

Burton, P. R., and Paige, J. L. (1981). Polarity of axonal microtubules in the olfactory nerve of the frog. Proc. Natl. Acad. Sci. USA *78*, 3269–3273.

Caceres, A., Banker, G. A., Steward, O., Binder, L., and Payne, M. (1984). MAP2 is localized to the dendrites of hippocampal neurons in culture. Dev. Brain Res. *13*, 314–318.

Carter, K. C., Taneja, K. L., and Lawrence, J. B. (1991). Discrete nuclear domains of poly-A mRNA and their relationship to the functional organization of the nucleus. J. Cell Biol. *115*, 1191–1202.

Davis, L., Banker, G. A., and Steward, O. (1987). Selective transport of RNA in hippocampal neurons in culture. Nature *330*, 477–479.

Dotti, C. G., Sullivan, C. A., and Banker, G. A. (1988). The establishment of polarity by hippocampal neurons in culture. J. Neurosci. *8*, 1454–1468.

Ferreira, A., Busciglio, J., and Caceres, A. (1989). Microtubule formation and neurite growth in cerebellar macroneurons which develop in vitro. Dev. Brain Res. *49*, 215–228.

Forscher, P., and Smith, S. J. (1988). Actions of cytochalasins on the organization of actin filaments and microtubules in a neuronal growth cone. J. Cell Biol. *107*, 1505–1516.

Garner, C. C., Tucker, R. P., and Matus, A. (1988). Selective localization of mRNA for cytoskeletal protein MAP2 in dendrites. Nature *336*, 674–679.

Goldman, R. D. (1971). The role of three cytoplasmic fibers in

BHK-21 cell motility: microtubules and the effects of colchicine. J. Cell Biol. *51*, 752–762.

Goldschmidt, R. B., and Steward, O. (1982). Neurotoxic effects of colchicine: differential susceptibilty of CNS neuronal populations. Neuroscience *7*, 695–714.

Goslin, K., and Banker, G. (1991). Culturing Nerve Cells (London, England: MIT Press).

Heidemann, S. R., Landers, J. M., and Hamborg, M. A. (1981). Polarity orientation of axonal microtubules. J. Cell Biol. *91*, 661–665.

Hesketh, J. E., and Pryme, I. F. (1991). Interaction between mRNA, ribosomes and the cytoskeleton. Biochem. J. *277*, 1–10.

Hillman, D. H. (1988). Dendritic shape and structural determinants. In Intrinsic Determinants of Neuronal Form and Function (New York: Alan R. Liss, Inc.).

Hirokawa, N., Hisanaga, S. I., and Shiomura, Y. (1988). MAP2 is a component of crossbridges between microtubules and neurofilaments in the neuronal cytoskeleton: quick freeze, deep-etch immunoelectron microscopy and reconstitution studies. J. Neurosci. *8*, 2769–2779.

Horne, S., and Hesketh, J. (1990). Immunological localization of ribosomes in striated rat muscle. Biochem. J. *268*, 237–240.

Jirikowski, G. F., Sanna, P. P., and Bloom, F. E. (1990). mRNA coding for oxytocin is present in axons of the hypothalamoneurohypophysial tract. Proc. Natl. Acad. Sci. USA *87*, 7400–7404.

Kleiman, R., Banker, G., and Steward, O. (1990). Differential subcellular localization of particular mRNAs in hippocampal neurons in culture. Neuron *5*, 821–830.

Kosik, K. S., and Finch, E. A. (1987). MAP2 and tau segregate into dendritic and axonal domains after the elaboration of morphologically distinct neurites: an immunocytochemical study of cultured rat cerebrum. J. Neurosci. *7*, 3142–3153.

Lenk, R., Ransom, L., Kaufmann, Y., and Penman, S. (1977). A cytoskeletal structure with associated polyribosomes obtained from HeLa cells. Cell *10*, 67–78.

Letourneau, P. C., Shattuck, T. A., and Ressler, A. H. (1987). Pull and push in neurite elongation: observations on the effects of cytochalasin and taxol. Cell Motil. Cytoskel. *8*, 193–209.

Litman, P., Barg, J., Rindzoonski, L., and Ginzburg, I. (1993). Subcellular localization of tau mRNA in differentiating neuronal cell culture: implications for neuronal polarity. Neuron *10*, 627–638.

Matus, A., Bernhardt, R., and Hugh-Jones, T. (1981). High molecular weight MAPs are preferentially associated with dendritic microtubules in brain. Proc. Natl. Acad. Sci. USA *78*, 3010–3014.

Matus, A. R., Bernhardt, R., Bodmer, R., and Alaimo, D. (1986). MAP2 and tubulin are differentially distributed in the dendrites of developing neurons. Neuroscience *17*, 371–389.

Mohr, E., Fehr, S., and Richter, D. (1991). Axonal transport of neuropeptide encoding mRNAs within the hypothalamohypophysial tract of rats. EMBO J. *10*, 2419–2424.

Ornelles, D. A., Fey, E. G., and Penman, S. (1986). Cytochalasin releases mRNA from the cytoskeleton and inhibits protein synthesis. Mol. Cell. Biol. *6*, 1650–1662.

Pokrywka, N. J., and Stephenson, E. C. (1991). Microtubules mediate the localization of bicoid RNA during Drosophila oogenesis. Development *113*, 55–66.

Ramaekers, F. C., Benedetti, E. L., Dunia, I., Vorstenbosch, P., and Bloemendal, H. (1983). Polyribosomes associated with microfilaments in cultured lens cells. Biochim. Biophys. Acta *740*, 441–448.

Rao, A., and Steward, O. (1991). Evidence that protein constituents of postsynaptic membrane specializations are locally synthesized: analysis of proteins synthesized within synaptosomes. J. Neurosci. *11*, 2881–2895.

Sato-Yoshitake, R., Shiomura, Y., Miyasaki, H., and Hirokawa, N. (1989). Microtubule-associated protein 1B: molecular structure, localization, and phosphorylation-dependent expression in developing neurons. Neuron *3*, 229–238.

Schroder, H. C., Bernd, A., Zahn, R. K., and Muller, W. E. G. (1982). Interaction of polyribosomal components and polyribonucleotides with microtubule proteins. Mol. Biol. Rep. *8*, 233–237.

Schroder, H. C., Bernd, A., Zahn, R. K., and Muller, W. E. G. (1984). Binding of polyribonucleotides to microtubule proteins. Mech. Ageing Dev. *24*, 101–117.

Shaw, G., Banker, G., and Weber, K. (1985). An immunofluorescence study of neurofilament expression by developing hippocampal neurons in tissue culture. Eur. J. Cell Biol. *39*, 205–216.

Sheiness, D., and Darnell, J. E. (1973). Polyadenylic acid segment in the mRNA becomes shorter with age. Nature *241*, 265–268.

Singer, R. H. (1992). The cytoskeleton and mRNA localization. Curr. Opin. Cell Biol. *4*, 15–19.

Singer, R. H., Langevin, G. L., and Lawrence, J. B. (1989). Ultrastructural visualization of cytoskeletal mRNAs and their associated proteins using double label in situ hybridization. J. Cell Biol. *108*, 2343–2353.

Steward, O. (1983). Alterations in polysomes associated with dendritic spines during the reinnervation of the dentate gyrus of the adult rat. J. Neurosci. *3*, 177–188.

Steward, O. S., and Banker, G. A. (1992). Getting the message from the gene to the synapse: sorting and intracellular transport of RNA in neurons. Trends Neurosci. *15*, 180–186.

Steward, O., and Levy, W. B. (1982). Preferential localization of polysomes under the base of dendritic spines in granule cells of the dentate gyrus. J. Neurosci. *2*, 248–291.

Sundell, C. L., and Singer, R. H. (1991). Requirement of microfilaments in sorting of actin mRNAs. Science *253*, 1275–1277.

Taneja, K. L., Lifshitz, M., Fay, F. S., and Singer, R. H. (1992). Poly(A) RNA codistribution with microfilaments: evaluation by in situ hybridization and quantitative digital imaging microscopy. J. Cell Biol. *119*, 1245–1260.

Vale, R. D. (1992). Microtubule motors: many new models off the assembly line. Trends Biochem. Sci. *17*, 300–304.

Yisraeli, J. K., Sokol, S., and Melton, D. A. (1990). A two-step model for the localization of maternal mRNA in Xenopus oocytes: involvement of microtubules and microfilaments in the translocation and anchoring of Vg1 mRNA. Development *108*, 289–298.